

⁶⁸Ga-DOTA Positron Emission Tomography for Diagnosis of Spinal Cerebrospinal Fluid Leaks

Petros Evangelou, MD¹; Mohamed Aymen Omrane, PhD²; Johannes Thurow, MD²; Michael Mix, PhD²;
Christian Fung, MD¹; Niklas Lützen, MD³; Ganna Blazhenets, PhD²; Horst Urbach, MD³;
Jürgen Beck, MD^{1*} and Philipp T. Meyer, MD, PhD^{2*}

¹Department of Neurosurgery, Medical Center – University of Freiburg, Faculty of Medicine, University of Freiburg, 79106 Freiburg, Germany

²Department of Nuclear Medicine, Medical Center – University of Freiburg, Faculty of Medicine, University of Freiburg, 79106 Freiburg, Germany

³Department of Neuroradiology, Medical Center – University of Freiburg, Faculty of Medicine, University of Freiburg, 79106 Freiburg, Germany

*both authors contributed equally

First Author:

Petros Evangelou, MD
Department of Neurosurgery
Medical Center – University of Freiburg
Breisacher Straße 64
79106 Freiburg, Germany
Phone: +49 761 270-50010
Fax: +49 761 270-50800
petros.evangelou@uniklinik-freiburg.de

Corresponding Author:

Philipp T. Meyer, MD, PhD
Department of Nuclear Medicine
Medical Center – University of Freiburg
Hugstetter Straße 55
79106 Freiburg, Germany
Phone: +49 761 270-39160
Fax: +49 761 270-39300
philipp.meyer@uniklinik-freiburg.de

Word Count: 5293

Running Title: Ga-DOTA CSF-PET

ABSTRACT

Spontaneous intracranial hypotension (SIH) due to spinal cerebrospinal fluid (CSF) leakage causes substantial disease burden. In many patients, the course is protracted and refractory to conservative treatment, requiring targeted therapy. We propose positron emission tomography (PET) of the CSF space with ^{68}Ga -DOTA as a state-of-the-art approach of radionuclide cisternography (RC) and validate its diagnostic value.

Methods: Retrospective analysis of patients with suspected intracranial hypotension due to spinal CSF leaks who underwent whole-body PET/CT at 1, 3 and 5 hours after intrathecal lumbar injection of ^{68}Ga -DOTA. Two independent raters blinded to clinical data analyzed all scans by for direct and indirect RC signs of CSF leakage. Volume of interest analysis was performed to assess the biological half-life of the tracer in CSF space ($T_{1/2,\text{biol}}$) and the ratio of decay-corrected activity in CSF space at 5 and 3 hours (R5/3; simplified marker of tracer clearance). Comprehensive stepwise neuroradiological work-up served as reference, which was additionally validated by surgical findings and follow-up.

Results: Of 40 consecutive patients, 39 patients with a working diagnosis of intracranial hypotension due to a spinal CSF leak (n=31 spontaneous and n=8 post-interventional) could be analyzed. A spinal CSF leak was verified by the neuroradiological reference method in 18 of 39 patients. As the only direct and indirect diagnostic signs, extrathecal tracer accumulation at the cervicothoracic junction and lack of activity over the cerebral convexities (5h) showed a high diagnostic value for spinal CSF leaks (sensitivity/specificity: 67%/90% and 94%/67%, respectively). Their combination provided little improvement (71%/95%). Additional quantitative analyses yielded no benefit ($T_{1/2,\text{biol}}$: 94%/53%; R5/3: 94%/58%). Of note, the location of direct signs (extrathecal tracer accumulation) did not correlate with verified sites of spinal CSF leakage.

Conclusions: We propose CSF-PET with ^{68}Ga -DOTA as a novel, fast and convenient approach of RC for verification, though not localization, of spinal CSF leaks with high sensitivity and specificity. CSF-PET may fulfill an important gatekeeper function to stratify patients towards escalation (rule-in) or de-escalation

(rule-out) of diagnostic and therapeutic measures. Further prospective studies are needed to validate the present results and the potential of the methods to reduce the burden to the patient.

Key Words: radionuclide cisternography; spontaneous intracranial hypotension; PET.

INTRODUCTION

Spontaneous intracranial hypotension (SIH) is an increasingly recognized condition caused by spinal leakage of cerebrospinal fluid (CSF) (1). The clinical picture can be very diverse, especially in individuals with chronic disease, making the diagnosis of SIH difficult (2). Despite its name, it is reported that only 34%-50% of the patients show a low opening pressure upon lumbar puncture (2,3). Postural headache and either the presence of stereotypical imaging signs or an opening pressure < 6 cm H₂O are required for the diagnosis (4). Despite conservative therapy (bed rest, caffeine) and epidural blood patches (EBP), symptoms persist in 10-30% of patients warranting verification and localization of leakage to allow for targeted treatment (2,5). Typical diagnostic algorithms propose a combination of different imaging modalities including, often repetitive, digital subtraction myelography (1), that miss a substantial fraction of leaks (45-74%) (3). Considering their invasive nature and possible extensive radiation exposure (6) it is desirable to select patients with a high likelihood for a leak before escalating the diagnostic work-up.

The unsurpassed measurement sensitivity of radionuclide imaging techniques and the ability to repeat imaging for hours without causing additional radiation burden, underline the potential of radionuclide cisternography (RC) in this setting. After seminal reports (e.g. (7)) and introduction of ¹¹¹In-DTPA (8) and ^{99m}Tc-DTPA (9), RC gained rapid acceptance in the field, being considered the diagnostic “gold-standard” over years for proof and localization of CSF leaks (10-13). Common criticisms of RC, however, include poor image quality and spatial resolution, low sensitivity and specificity, lack of standardization and long examination (up to 48h). Despite methodological improvements like cross-sectional imaging with single-photon emission computed tomography (SPECT) (14) and hybrid SPECT/computed tomography (CT) (15) and quantitative analysis (10,13,16,17) RC was removed as diagnostic imaging tool from the International Classification of Headache Disorders, 3rd-edition (4). To date, RC is still commonly performed as planar scintigraphic imaging without taking advantage of state-of-the-art imaging like positron emission tomography (PET)/CT which offers improved sensitivity, spatial resolution, and quantification. In fact, CSF-PET was proposed 40 years ago using ⁶⁸Ga-EDTA (14), but has only rarely been applied in single cases (e.g., ⁶⁴Cu-DOTA) (18).

Against this background, the present study proposes a convenient CSF-PET methodology and validates its diagnostic value concerning the presence and localization of spinal CSF leak.

MATERIALS AND METHODS

Patients

The institutional review board approved this study and all subjects gave written informed consent to the examination and the retrospective analysis. Forty consecutive patients referred for CSF-PET with suspected intracranial hypotension due to a spinal CSF leak between Mai 2020 and March 2021 were eligible, of whom $n=39$ could be included (see Results).

Reference Standard

Patients underwent standard work-up including, often repeated, cranial and spinal MR-imaging, Gd-MR-myelography and digital subtraction myelography/CT-myelography. Please see Supplement for details.

Demonstration of a spinal CSF leak by comprehensive neuroradiological imaging defined positivity of the target condition (spinal CSF leak) and its localization. This entails a stepwise approach aiming at localizing or excluding a spinal CSF leak by dynamic digital subtraction myelography followed by dynamic CT-myelography in prone or lateral decubitus position (*I*). The result served as reference for definition of true positive, true negative, false positive and false negative results of various PET outcome measures for presence or absence of a spinal CSF leak (index test). In patients with verified CSF leaks, localizations provided by the reference method and PET (direct signs) were directly compared. Surgical findings (genuine “gold standard”, but only applicable in those with positive target condition) and clinical follow-up data were also assessed.

PET Acquisition

PET/CT scans (with low-dose or ultra-low-dose CT) covering the entire CSF space were acquired on a fully digital PET/CT system (Vereos, Philips Healthcare, The Netherlands) at 1, 3 and 5 hours after lumbar intrathecal injection of ^{68}Ga -DOTA (45-50MBq in 0.5-1.0ml). The preparation of ^{68}Ga -DOTA and the acquisition protocol are described in detail in the Supplement.

Visual PET Reads

Two experienced Nuclear Medicine physicians, blinded to all other clinical and diagnostic data as well as the results of quantitative PET analyses, evaluated all ^{68}Ga -DOTA-PET scans independently. Using the 1-h, 3-h and 5-h PET/CT datasets, visual reads of direct and indirect RC signs and a summary rating were done using a 3-step scale (0, none; 1, questionable/mild signal; 2, strong signal) (see Supplement for details):

Directs signs of spinal CSF leak include uni- or bilateral extrathecal tracer accumulation, witnessed at least at one time point, which was localized according to 28 spinal segments. In case of extrathecal tracer accumulation on multiple consecutive segments, these were rated in combination, assuming that they stem from the same process.

Indirect signs of spinal CSF leak include radiotracer accumulation in the bladder (1h) and radiotracer accumulation in the basal cisterna and over the cerebral convexities. In addition, iatrogenic tracer extravasation at the injection site was assessed.

Finally, a 3-step summary rating was independently recorded by each rater for each individual case (0, 1 and 2 for no, questionable/possible and probable CSF leakage, respectively). After discussion of discrepant cases, the raters reached a consensus.

Quantitative PET Analysis

The time course of total radioactivity within the CSF space was characterized in terms of biological half-life ($T_{1/2,\text{biol}}$) and, as a simplified approach, using the ratio of total radioactivity within the CSF space at 5 and 3 h (R5/3; decay-corrected data). Volume of interest analyses were performed after co-registration of all three PET/CT scans in each patient (Supplement).

Please see Supplement for statistical analyses.

RESULTS

Patient Characteristics

Forty consecutive patients (age 46.2 ± 14.1 years, 32/8 females/males) were eligible. Thirty-two patients were diagnosed with SIH (4) (in one patient spinal puncture failed, leaving $n=31$), $n=4$ with possible persistent/relapsing CSF leak after previous open surgical treatment for SIH and $n=4$ with questionable SIH, in whom a former lumbar puncture or peridural anaesthesia was assumed to be causal by the referring doctor. In 37 of 39 (95%) included patients a follow-up of 3.6 ± 2.5 months was available. CSF-PET was well tolerated by all patients. There were no side-effects except those commonly associated with lumbar puncture.

In 18 of 39 (46%) patients a spinal CSF leak could be localized by stepwise neuroradiological imaging, located on C7 to T3 ($n=6$) or T7 to L1 ($n=12$) (Supplemental Figure 1). CSF leaks were only verified in patients with SIH without previous surgery or alternative causes (detection rate 18/31, 58%). In $n=12$ a ventral dural tear was found (coinciding with a microspur on surgery in $n=9$), while a lateral leak and a direct CSF-venous fistula were diagnosed in $n=3$ each. Except for one patient, who refused surgery and was successfully treated by untargeted EBP (untargeted), all patients with proven leaks underwent surgery with symptom improvement ($n=10$) or resolution ($n=6$) in 16 of 17 patients (94%). In the remaining case, a 60-year-old male with long-standing symptoms, cerebral MRI findings of SIH markedly improved while symptoms remained unchanged. In turn, 15 of 21 patients, in whom no leak could be identified, were treated by EBP. Follow-up data was available in 14 of these 15 patients (27 EBP in total), showing an improvement or resolution of symptoms in only 2 cases each (response 4/14, 29%). The remaining patients either refused treatment or received alternative diagnoses and treatments. Taken together, clinical outcome strongly supports the validity of the neuroradiological reference standard.

Visual PET Reads

Visual reads (examples in Figures 1-3 and Supplemental Figure 2) of direct signs of a spinal CSF leak were highly consistent between both raters (agreement in 86% of ratings; Supplement). Supplemental

Figure 1 summarizes the sites of extrathecal tracer accumulation. The findings cluster at the craniocervical and cervicothoracic junction (Figure 3), over the lower thoracic spine and in the lumbosacral region (Supplemental Figure 1). To further reduce the data, we assorted all sites of extrathecal tracer accumulation to these regions (selecting the most prominent if >1 site) (Table 1). Extrathecal tracer accumulation at the craniocervical junction and the cervicothoracic junction showed no significant dependency on scan time, whereas those in the lower thoracic spine and in the lumbosacral region significant decreased with time (Supplement).

Mean ratings (across raters and scans) of direct signs at the lower thoracic spine and in the lumbosacral region did not differ between patients without and with verified spinal CSF leak, while there was a highly significant difference in the cervicothoracic junction between both groups allowing for an accurate diagnostic separation of groups (*AUC ROC* 0.81; sensitivity/specificity 67%/90%, cut-off 0.33, i.e. mild extrathecal tracer accumulation in at least one scan; Table 1). Extrathecal tracer accumulation at the craniocervical junction was rarely observed (3/39) and occurred only in patients with verified spinal CSF leak ($p=0.055$). Of note, there was no obvious association between the location of verified spinal CSF leaks and extrathecal tracer accumulation on PET. In fact, sites of extrathecal tracer accumulation usually extended over multiple segments and overlapped with the site of verified leak in only 3 of 18 cases (locations differed by only 1 and >1 segment in $n=3$ and $n=12$, respectively) (Supplemental Figure 1).

Ratings of indirect signs of CSF leakage and tracer extravasation at the injection site were also highly consistent between observers (agreement in 80-85% of ratings; Supplement). Ratings of the basal cisterna and tracer accumulation over the cerebral hemispheres showed a significant increase with time and dependence on presence/absence of a spinal CSF leak while tracer extravasations at the injection site significantly decreased with time (Supplement).

The only indirect sign that showed a highly significant difference between patients without and with verified spinal CSF leak was lack of tracer accumulation over the cerebral hemispheres in the 5-h scan, which allowed for an accurate diagnostic group separation (*AUC ROC* 0.79; sensitivity/specificity

94%/67%, cut-off >1.0, i.e. more than only mild tracer accumulation over the cerebral hemispheres at 5 hours; Table 1).

Both raters also filed a summary score considering all direct and indirect signs, which was highly consistent between raters (agreement in 77% of cases; Supplement). The consensus rating of both raters yielded a highly significant group difference between patients without and with verified spinal CSF leak (Table 1; 0.43 ± 0.68 vs. 1.39 ± 0.78 , $p=0.0006$, $AUC\ ROC=0.80$, sensitivity/specificity 83%/67%, cutoff 1).

Similar results were gained when analyses were restricted to patients with SIH without previous surgery or alternative causes (Supplemental Table 1).

Quantitative PET Analysis

In 2 patients quantification was omitted because of partially epidural tracer injection and out-of-field of view artefacts (both scans were still read visually). As expected, $T_{1/2,biol}$ and R5/3 were highly correlated ($\rho=0.94$, $p<0.0001$). $T_{1/2,biol}$ and R5/3 showed no significant association with age, sex, body weight or body height, neither in the entire group nor in the groups with and without verified spinal CSF leak. However, $T_{1/2,biol}$ and R5/3 were significantly smaller in patients with than without spinal CSF leak (Table 1), allowing for a diagnostic group separation ($T_{1/2,biol}$: $AUC\ ROC=0.70$, sensitivity/specificity 94%/53%, cut-off <7.9h; R5/3: $AUC\ ROC=0.78$, sensitivity/specificity 94%/58%, cut-off <0.82).

Combination of Qualitative and Quantitative Analyses

We used stepwise forward regression, including aforementioned significant parameters with the exception of $T_{1/2,biol}$ (highly correlated to R5/3) to explore which combined parameters best predict a spinal CSF leak. Minimum Akaike Information Criterion (36.3) was reached by retaining extrathecal tracer accumulation at the cervicothoracic junction and lack of tracer accumulation over the cerebral hemispheres (resulting multi-nominal logistic regression model: $AUC\ ROC=0.88$, sensitivity/specificity 71%/95%).

DISCUSSION

We propose CSF-PET using ^{68}Ga -DOTA as a novel, state-of-the-art approach of RC, which provides several possible advantages over conventional RC. By employing a very rigorous diagnostic reference standard in an exceptional large cohort of patients, we were able not only to validate the diagnostic accuracy of CSF-PET for verifying, though not localizing, spinal CSF leakage, but also to unravel several misconceptions and controversies concerning RC.

PET provides superior spatial resolution (2-3 times higher) and sensitivity (2-3 magnitudes higher) compared to scintigraphy and SPECT (19) which allows detecting and quantifying the slow cephalad ascent of CSF even with short-lived radionuclides. The entire examination is completed within 5-6 hours in contrast to conventional RC, which often takes up to 48 hours. In addition, individual PET scans are acquired within 20-30 min, which compares favorably with whole-body SPECT/CT examinations that may take up to 1 h. The estimated dose for CSF-PET with ^{68}Ga -DOTA is approximately 1.24 mGy/MBq for the spinal cord (highest organ dose) and 0.16 mSv/MBq effective dose equivalent, which is slightly higher than for ^{111}In -DTPA (0.95 mGy/MBq and 0.14 mSv/MBq, respectively; assuming the same biokinetic model for both tracers (normal $T_{1/2,\text{biol}}$) and accounting for differences in energy transfer and physical half-lives) (20). Thus, for a typical injected dose of 37 MBq ^{68}Ga -DOTA, the estimated effective dose is 5.9 mSv. CT scans add about 3-4 mSv, which may be further reduced with dose-sparing techniques. The fast decay of ^{68}Ga -DOTA (as opposed to ^{111}In -DOTA) also implies there is no relevant radiation exposure to medical personnel if patients undergo spinal surgery briefly after diagnostics (often on the following day at our institution). Of note, the synthesis and quality control of ^{68}Ga -DOTA is also very simple and readily available at most larger centers (at least in Europe), rendering it a convenient alternative to ^{111}In -DTPA. Finally, the high image quality of PET/CT scans renders CSF-PET with ^{68}Ga -DOTA much more appealing and convincing than conventional RC, which in our experience strongly improves the acceptance of RC in clinical routine.

The average $T_{1/2,\text{biol}}$ of patients without verified leakage ($9.5\pm 7.0\text{h}$) is somewhat lower but still in line with the literature ($13.5\pm 4.5\text{h}$) (10), considering that this group possibly includes subjects with missed

or iatrogenic leaks. We propose $R5/3$ as simpler estimate of tracer clearance, which circumvents the need for an 1-h scan and exponential fitting and yielded a slightly higher diagnostic performance. However, quantitative analyses provided no additional benefit over visual reads, which is in line with findings in conventional RC (21). Still, we routinely perform quantification as simple adjunct to visual reads that may be particularly valuable for follow-up assessments (10).

A particular strength of the present study is the use of a rigorous neuroradiological reference standard that was additionally validated by surgical findings and outcome. To the best of our knowledge, no previous study on RC included more patients with appropriate verification (e.g., in the seminal work by Schievink et al. (22) correlation of RC with CT myelography and surgery is only available in 8 and 4 of 11 patients, respectively), with earlier studies often using response to EBP as reference (10,16,23,24). However, given the uncertainty about the efficacy and mechanism of action of EBP (e.g., success sometimes only after several attempts, targeted vs. non-targeted EBP, often only short-term efficacy, possible placebo effects) (25), as well as the current, improved understanding of SIH pathophysiology (see below) (3,26-28), we are convinced that the present reference is most appropriate. We were able to verify a spinal CSF leak in 18 of 31 (58%) patients with SIH without previous surgery or alternative causes. Albeit few spinal leaks may have been missed (see below), this fraction is in line with the literature (3) and underlines the uncertainty associated with the clinical diagnosis of SIH, which does not require verification of a leak (4).

We made several important observations: First, the site of extrathecal tracer accumulation on CSF-PET is not related to the actual location of leakage. This has not been systematically shown before. We do not believe that this is related to the tracer used (e.g., later detection of actual sites of leakage with longer-lived isotopes) but assume that this finding represents a general shortcoming of RC. In fact, patterns observed in this study and described in the literature are very similar. However, unlike earlier studies, we used a rigorous diagnostic reference standard that is a prerequisite for detecting this mismatch. Second, ^{68}Ga -DOTA-PET like conventional RC (10,12,13,17,24) may show several sites of extrathecal tracer accumulation, which, however, do not indicate that there are multiple leaks but rather that the tracer leaves

the spinal epidural space at multiple locations. This in line with the current concept that spontaneous spinal CSF leaks most commonly occur in the lower cervical and thoracic spine (22,26), being frequently caused by well-defined singular lesions (e.g., dural tears due to discogenic microspur) (3,26,27). This is also reflected by current excellent surgical outcomes. Third, lumbar/lumbosacral extrathecal tracer accumulations are very rarely (if ever) indicative of leaks in that region but are usually of iatrogenic origin instead, albeit being frequently reported in the RC literature (10,23). Fourth, early bladder activity as an indirect sign possesses little (if any) diagnostic value, which contrasts with early RC reports (11) but agrees with more recent studies (17,21). Fifth, the term *direct sign* for extrathecal tracer accumulation to the paraspinal space in RC is most likely misleading. In fact, the only *direct signs* associated with verified leaks in the present study are probably RC equivalents of cervicothoracic extrathecal fluid accumulation on X-ray myelography, commonly referred to as *false localizing sign* (29). We assume that this is simply due to anatomic reasons (e.g., more flexible spinal alignment). To the best of our knowledge, there are no other systematic studies available providing a detailed (segmental) comparison of neuroradiological or surgical and RC findings. Even in the aforementioned seminal work (22), anatomical description of CT myelography or RC findings do not pinpoint locations of actual leaks but only give approximate segmental heights or ranges of extrathecal findings. Given the rapid epidural spread and uncertain mechanism of action of EBP (see above), a therapeutic response to EBP can hardly be taken as a confirmation of an apparent leak localization given by RC as frequently done in the literature (22-24).

CSF-PET shows high diagnostic performance in a particularly challenging clinical situation: Extrathecal tracer accumulation at the cervicothoracic junction provides a high diagnostic specificity (90%), though only moderate sensitivity (67%) for verification of spinal CSF leaks. The latter fits to the observation that direct signs of CSF leakage on conventional RC might be absent in a highly variable fraction of patients with SIH (10-70%) (13,22-24). In turn, indirect signs of CSF leak on conventional RC are found in the vast majority (>90%) of patients (11,13,22,24). Lack of tracer appearance over the cerebral convexities in the 5-h scan provides a very high sensitivity (94%) at moderate specificity (67%). A very high sensitivity of this sign was also suggested by conventional RC studies (13,17,21). The summary rating of both raters was

motivated by clinical practice with conventional RC and comprised all direct and indirect signs (including those of no or little value) with a weighting left to the discretion and experience of the rater. Thus, it is not surprising that this consensus read did not perform superior to a combination of both aforementioned features by logistic regression.

Given the considerable rate of negative findings of CT and MRI myelography in SIH (45-74%) (3), it is interesting to note that 4 of 14 patients (29%) with negative neuroradiological imaging and treated by EBP showed a clinically relevant response to EBP. All four patients fall into the groups of patients judged to show “questionable/possible” and “probable” (n=2 each) signs of spinal CSF leak but in whom no leak could be verified (Supplemental Figures 1 and 2). Aside from direct and indirect signs suggestive of spinal CSF leaks (in 3 and 1 patients, respectively), all four patients also showed below-threshold $T_{1/2, \text{biol}}/R5/3$ values. Thus, it is tempting to speculate that these patients represent false-negative cases on neuroradiological imaging, leading to an underestimation of the true sensitivity of CSF-PET.

In light of these observations, the clinical role of CSF-PET is clearly not to localize the site of spinal CSF leak. It may, however, play an essential role in verifying spinal CSF leakage with high sensitivity (to rule-out) or specificity (to rule-in), depending on clinical need. For instance, extrathecal tracer accumulation at the cervicothoracic junction is most likely associated with a spinal CSF leak (specificity 90%) and may prompt additional examinations. In turn, sufficient tracer accumulation over the cerebral convexities strongly argues against a spinal CSF leak (sensitivity >90%) leading to a defensive approach (see also (21)). One motivation would clearly be to minimize the exposure to ionizing radiation in this predominately young and female population: Patients usually present with a long disease history of months to years, having already undergone a plethora of diagnostic and therapeutic actions. In the present sample, on average two combined digital subtraction myelographies/CT-myelographies were performed per patient in our institution only. The resulting median radiation exposure can be estimated to be about 52.6mSv per patient in the present sample (6), or, in other words, to cause 1 additional radiation-induced cancer death in 250-500 patients (30). This risk may be substantially reduced by including a gatekeeper examination.

Limitations of the present study include its retrospective nature, which warrants prospective validation. In particular, a direct comparison of CSF-PET to conventional RC would be desirable (e.g., by co-injection of tracers). Furthermore, the limited number of cases did not allow for detailed contemplation of interesting subgroups (e.g. SIH vs. non-SIH, type of leakage). Finally, the present study summarized the first patients examined with this novel methodology that was developed in parallel. By retrospectively analyzing this set of patients at once in a strictly blinded fashion, we minimized possible effects of the raters' learning curves and bias. However, optimal technical aspects still need to be defined. For instance, these include measures to avoid iatrogenic extrathecal tracer accumulation. Moreover, albeit earlier studies showed that upright positioning or exercise does not affect CSF circulation under normal conditions (7), a preliminary report of two cases suggests that a sitting position may improve the detection rate of spinal CSF leaks (31). Further studies are needed to explore if such efforts or other technical refinements can increase the rate of CSF leakage and improve the detection and possibly localization of spinal CSF leaks by PET.

CONCLUSION

We propose CSF-PET with ^{68}Ga -DOTA as a novel, fast and convenient approach of RC for verification, though not localization, of CSF-leaks with high sensitivity and specificity. CSF-PET may fulfill an important gatekeeper function to stratify patients towards escalation (rule-in) or de-escalation (rule-out) of diagnostic and therapeutic measures. Further prospective studies are needed to validate the present results and the potential of the methods to reduce the burden to the patient.

DISCLOSURES

The authors report no competing interests.

KEY POINTS

Question: Proposal and validation of cerebrospinal fluid (CSF) PET with ^{68}Ga -DOTA for diagnosis of spinal CSF leakage with reference to comprehensive, stepwise neuroradiological imaging.

Pertinent Findings: The present retrospective study included 39 consecutive adults with suspected intracranial hypotension who underwent ^{68}Ga -DOTA CSF-PET. Extrathecal tracer accumulation at the cervicothoracic junction and lack of activity over the cerebral convexities (at 5 hours) showed a high diagnostic value for spinal CSF leaks (sensitivity/specificity: 67%/90% and 94%/67%, respectively).

Implications for Patient Care: CSF-PET with ^{68}Ga -DOTA may serve as a gatekeeper to stratify patients towards escalation or de-escalation of further diagnostic and therapeutic measures and, thus, reduce the burden to the patient.

REFERENCES

1. Luetzen N, Dovi-Akue P, Fung C, Beck J, Urbach H. Spontaneous intracranial hypotension: diagnostic and therapeutic workup. *Neuroradiology*. 2021;63:1765-1772.
2. Beck J, Häni L, Ulrich CT, et al. Diagnostic challenges and therapeutic possibilities in spontaneous intracranial hypotension. *Clinical and Translational Neuroscience*. 2018;2:1-11.
3. Kranz PG, Gray L, Amrhein TJ. Spontaneous Intracranial Hypotension: 10 Myths and Misperceptions. *Headache*. 2018;58:948-959.
4. IHS. Headache Classification Committee of the International Headache Society (IHS) The International Classification of Headache Disorders, 3rd edition. *Cephalalgia*. 2018;38:1-211.
5. Schievink WI, Maya MM, Jean-Pierre S, Nuno M, Prasad RS, Moser FG. A classification system of spontaneous spinal CSF leaks. *Neurology*. 2016;87:673-679.
6. Nicholson PJ, Guest WC, van Prooijen M, Farb RI. Digital Subtraction Myelography is Associated with Less Radiation Dose than CT-based Techniques. *Clin Neuroradiol*. 2021;31:627-631.
7. Dichiro G. Movement of the Cerebrospinal Fluid in Human Beings. *Nature*. 1964;204:290-291.
8. Hosain F, Som P. Chelated ¹¹¹In: an ideal radiopharmaceutical for cisternography. *Br J Radiol*. 1972;45:677-679.
9. Som P, Hosain F, Wagner HN, Jr., Scheffel U. Cisternography with chelated complex of ^{99m}Tc. *J Nucl Med*. 1972;13:551-553.
10. Moriyama E, Ogawa T, Nishida A, Ishikawa S, Beck H. Quantitative analysis of radioisotope cisternography in the diagnosis of intracranial hypotension. *J Neurosurg*. 2004;101:421-426.
11. Morioka T, Aoki T, Tomoda Y, et al. Cerebrospinal fluid leakage in intracranial hypotension syndrome: usefulness of indirect findings in radionuclide cisternography for detection and treatment monitoring. *Clin Nucl Med*. 2008;33:181-185.
12. Takahashi K, Mima T. Cerebrospinal fluid leakage after radioisotope cisternography is not influenced by needle size at lumbar puncture in patients with intracranial hypotension. *Cerebrospinal Fluid Res*. 2009;6:5.
13. Hoshino H, Higuchi T, Achmad A, Taketomi-Takahashi A, Fujimaki H, Tsushima Y. A new approach for simple radioisotope cisternography examination in cerebrospinal fluid leakage detection. *Ann Nucl Med*. 2016;30:40-48.
14. Bergstrand G, Larsson S, Bergstrom M, Eriksson L, Edner G. Cerebrospinal fluid circulation: evaluation by single-photon and positron emission tomography. *AJNR Am J Neuroradiol*. 1983;4:557-559.
15. Novotny C, Potzi C, Asenbaum S, Peloschek P, Suess E, Hoffmann M. SPECT/CT fusion imaging in radionuclide cisternography for localization of liquor leakage sites. *J Neuroimaging*. 2009;19:227-234.

16. Horikoshi T, Ikegawa H, Uchida M, Takahashi T, Watanabe A, Umeda T. Tracer clearance in radionuclide cisternography in patients with spontaneous intracranial hypotension. *Cephalalgia*. 2006;26:1010-1015.
17. Sakurai K, Nishio M, Yamada K, et al. Comparison of the radioisotope cisternography findings of spontaneous intracranial hypotension and iatrogenic cerebrospinal fluid leakage focusing on chronological changes. *Cephalalgia*. 2012;32:1131-1139.
18. Freesmeyer M, Schwab M, Bestehar B, Grober S, Waschke A, Drescher R. High-Resolution PET Cisternography With ⁶⁴Cu-DOTA for CSF Leak Detection. *Clin Nucl Med*. 2019;44:735-737.
19. Cherry S, Sorenson J, Phelps M. *Physics in Nuclear Medicine, 4th Edition*: Saunders; 2012.
20. ICRP. Radiation Dose to Patients from Radiopharmaceuticals. *ICRP Publication 53 Ann ICRP*. 1988;18.
21. Mokri B. Radioisotope cisternography in spontaneous CSF leaks: interpretations and misinterpretations. *Headache*. 2014;54:1358-1368.
22. Schievink WI, Meyer FB, Atkinson JL, Mokri B. Spontaneous spinal cerebrospinal fluid leaks and intracranial hypotension. *J Neurosurg*. 1996;84:598-605.
23. Yoo HM, Kim SJ, Choi CG, et al. Detection of CSF leak in spinal CSF leak syndrome using MR myelography: correlation with radioisotope cisternography. *AJNR Am J Neuroradiol*. 2008;29:649-654.
24. Hyun SH, Lee KH, Lee SJ, et al. Potential value of radionuclide cisternography in diagnosis and management planning of spontaneous intracranial hypotension. *Clin Neurol Neurosurg*. 2008;110:657-661.
25. Hani L, Fung C, Jesse CM, et al. Outcome after surgical treatment of cerebrospinal fluid leaks in spontaneous intracranial hypotension-a matter of time. *J Neurol*. 2022;269:1439-1446.
26. Beck J, Ulrich CT, Fung C, et al. Diskogenic microspurs as a major cause of intractable spontaneous intracranial hypotension. *Neurology*. 2016;87:1220-1226.
27. Kranz PG, Gray L, Malinzak MD, Amrhein TJ. Spontaneous Intracranial Hypotension: Pathogenesis, Diagnosis, and Treatment. *Neuroimaging Clin N Am*. 2019;29:581-594.
28. Dobrocky T, Nicholson P, Hani L, et al. Spontaneous intracranial hypotension: searching for the CSF leak. *Lancet Neurol*. 2022;21:369-380.
29. Schievink WI, Maya MM, Chu RM, Moser FG. False localizing sign of cervico-thoracic CSF leak in spontaneous intracranial hypotension. *Neurology*. 2015;84:2445-2448.
30. UNSCEAR. *Report of the United Nations Scientific Committee on the Effects of Atomic Radiation 2010. Fifty-seventh session, includes Scientific Report: Summary of low-dose radiation effects on health 2010*.

31. Lu Y-Y, Wang H-Y, Lin Y, Lin W-Y. The Value of Changing Position in the Detection of CSF Leakage in Spontaneous Intracranial Hypotension Using Tc-99m DTPA Scintigraphy: Two Case Reports. *Iranian Journal of Radiology*. 2012;9:150-153.

Table 1: Results of Visual and Quantitative PET Analyses

Parameter		w/o leak (<i>n</i> =21)	w/ leak (<i>n</i> =18)	<i>p</i>	<i>ROC AUC</i>
Bladder activity	1h	1.21±0.68	1.42±0.55	n.s.	-
Basal cisterna	1h	1.31±0.64	1.53±0.62	n.s.	-
	3h	1.83±0.37	1.74±0.56	n.s.	-
	5h	1.81±0.37	1.71±0.56	n.s.	-
Cerebral convexities	1h	0.02±0.11	0.03±0.12	n.s.	-
	3h	0.71±0.49	0.50±0.59	n.s.	-
	5h	1.43±0.83	0.50±0.56	0.0016	0.79
Craniocervical (SO-C1)		0.00±0.00	0.19±0.47	(0.055)	(0.58)
Cervicothoracic (C6-T2)		0.06±0.20	0.68±0.58	0.0001	0.81
Lower thoracic (T7-T12)		0.32±0.63	0.44±0.64	n.s.	-
Lumbosacral (L2-S2)		0.75±0.74	0.79±0.81	n.s.	-
Consensus summary read		0.43±0.68	1.39±0.78	0.0006	0.80
PET quantification	T _{1/2,biol} [h]	9.47±7.03	4.54±2.45	0.0043	0.70
	R5/3	0.79±0.16	0.63±0.18	0.0023	0.78

Except for PET quantification (continuous data), all data represent 3-step ordinal scales with values giving mean values across readers and times (if not separated) or the consensus of raters. Given are mean values±standard deviation, *p*-values of statistical comparisons between patients without (w/o) and with (w/) spinal CSF leak (n.s., not significant, *p*-values in parenthesis indicate trend effects) and area under the receiver operating characteristics curve (*ROC AUC*; only for significant and trend effects). Anatomical localizations refer to sites of tracer accumulation (spinal segments; SO, suboccipital)

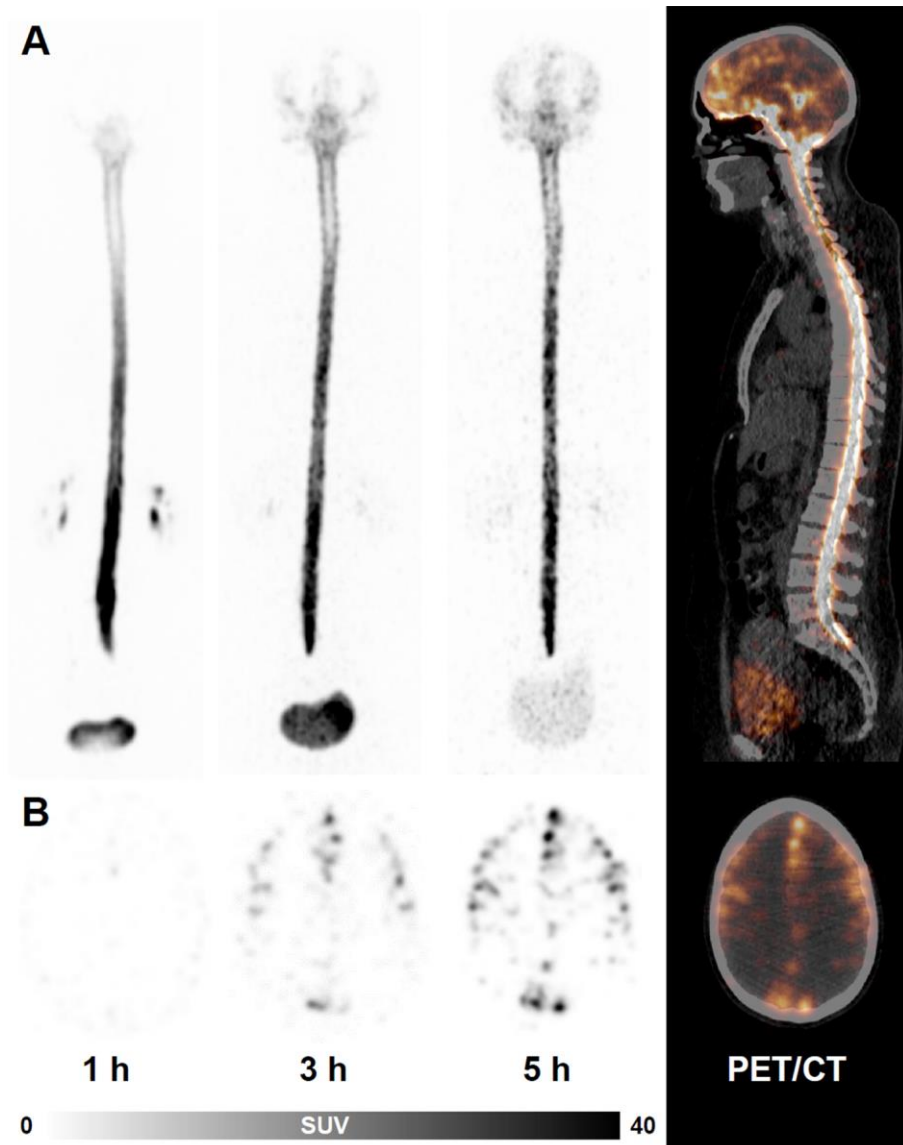


Figure 1: Normal CSF-PET in a patient without verified spinal CSF leak.

A, maximum intensity projections of PET (posterior view; scaled for optimal display) at 1h, 3h and 5h after injection of ^{68}Ga -DOTA and sagittal PET/CT fusion image (at 5h; far right). B, transaxial PET slices at the level of the centrum semiovale at 1h, 3h and 5h and a PET/CT fusion image (far right). Note the time-dependent cephalad ascent of the tracer with normal accumulation of activity over the cerebral hemispheres. The patient (No. 38) was treated with an epidural blood patch without response.

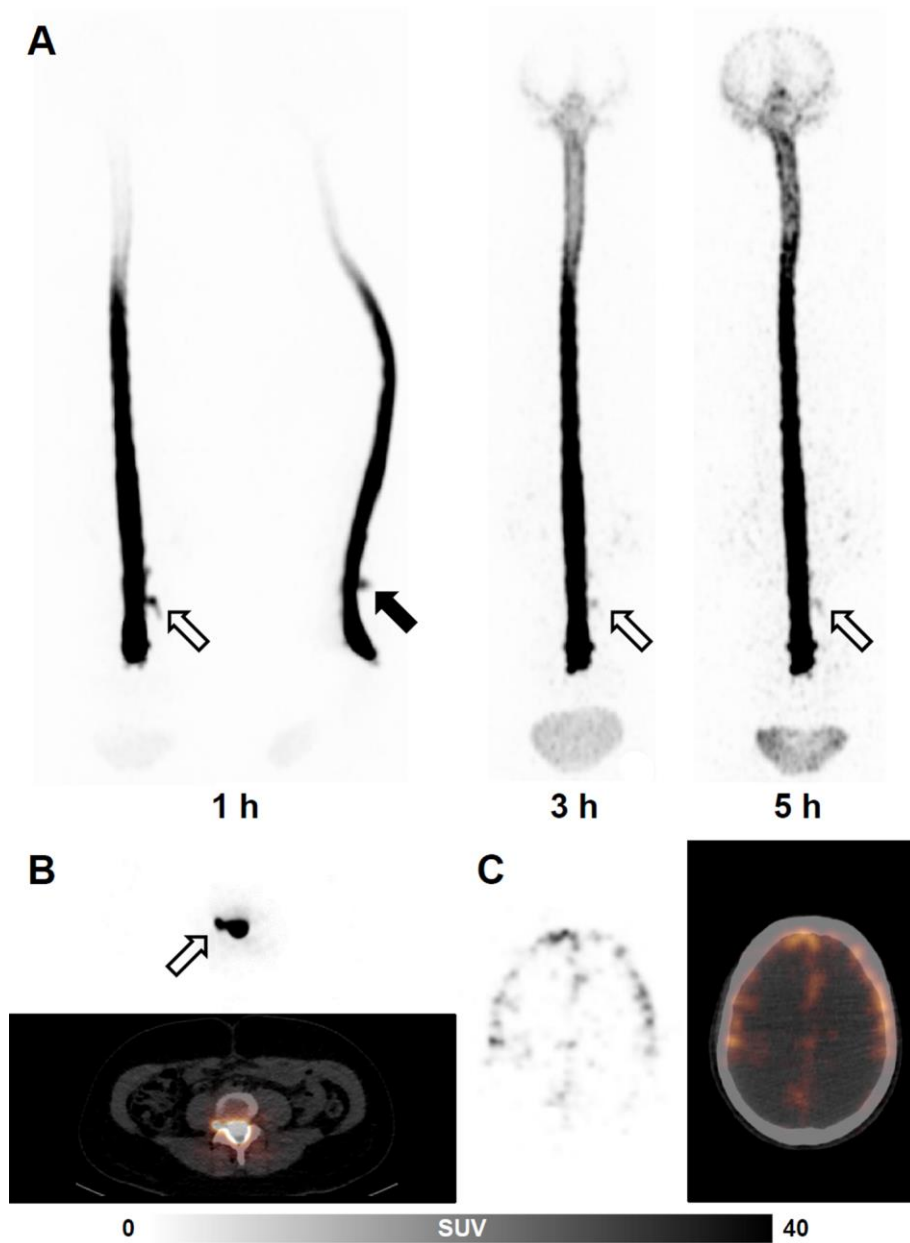


Figure 2: CSF-PET with iatrogenic extrathecal tracer accumulation in a patient without verified spinal CSF leak.

A, maximum intensity projections of PET at 1h, 3h and 5h (posterior view; at 1h also lateral view; scaled for optimal display) after injection of ^{68}Ga -DOTA. B and C, transaxial PET and PET/CT fusion images at the level of L3/4 (1h) and the centrum semiovale (5h), respectively. Despite there is strong iatrogenic egression of tracer in the trajectory of the injection needle (filled arrow) and to the right side at the level of L3/4 that vanishes with time (open arrow), the cephalad ascent of tracer is normal with tracer accumulation over the cerebral convexities. The patient (No. 15) was treated with an epidural blood patch without response.

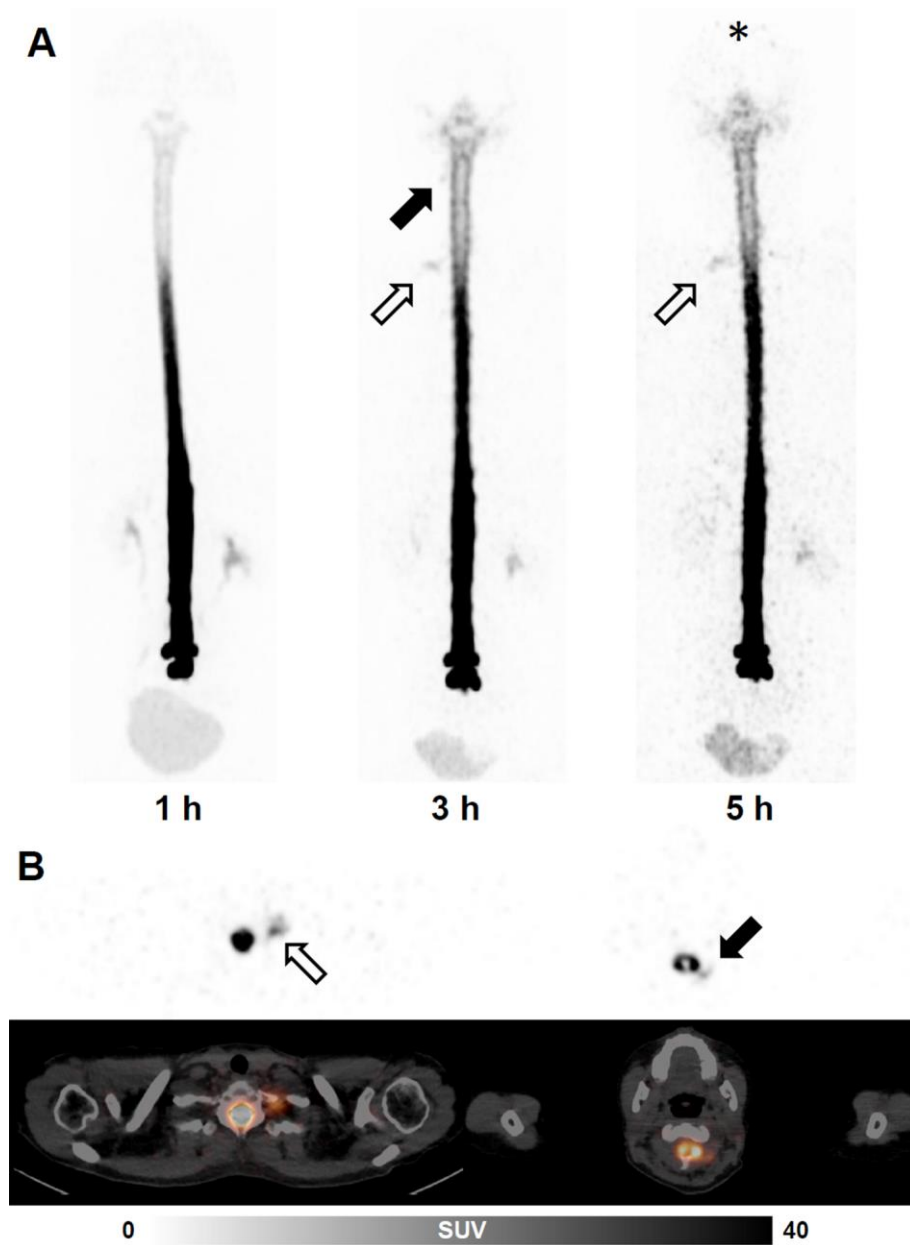
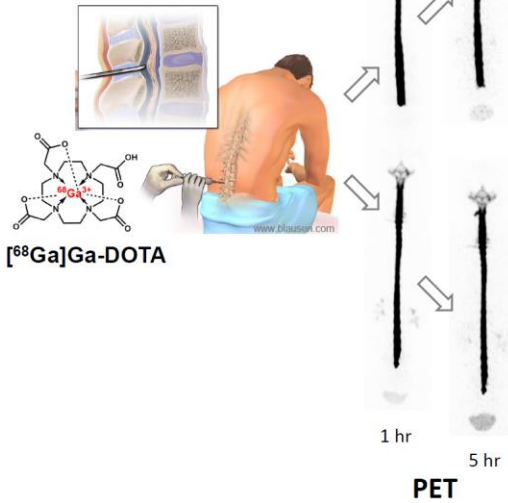


Figure 3: Pathological CSF-PET in a patient with verified spinal CSF leak.

A, maximum intensity projections of PET at 1h, 3h and 5h (posterior view; scaled for optimal display) after injection of ^{68}Ga -DOTA. B, transaxial PET and PET/CT fusion images at the level of C7/T1 and C2 (3h), respectively. Compatible with a surgically verified, lower thoracic lateral CSF leak, there are moderate and mild extrathecal tracer accumulations at the level of the cervicothoracic junction (open arrow) and in the upper cervical region (filled arrow), respectively. Note, that there is a lack of tracer accumulation over the cerebral convexities (asterisk). The patient (No. 27) was treated by surgery with improvement of symptoms.

Cerebrospinal fluid (CSF) leak?



normal tracer ascent
(no extra-dural tracer accumulation)
→ no CSF leak (rule-out)
→ de-escalation of diagnostics and therapy, alternative diagnosis?

(no tracer ascent)
extra-dural tracer accumulation
→ CSF leak (rule-in)
→ escalation of diagnostics and therapy, surgery?

Graphical Abstract

MATERIALS AND METHODS

Reference Standard

All patients underwent standard work-up including cranial and spinal MR imaging ($n = 40$), MR myelography ($n = 28$), digital subtraction myelography with subsequent CT myelography (DSM/CTM) ($n = 40$) and dynamic CSF testing using a computerized lumbar constant infusion ($n = 36$). Of note, numerous patients underwent repeated examination, which is of particular interest in case of DSM/CTM because of the high radiation exposure ($n = 15, 13, 10$ and 2 patients underwent $1, 2, 3$ and 4 DSM/CTM, respectively). All findings were presented to an interdisciplinary SIH Board including experienced physicians from the Departments of Neurosurgery, Neurology and Neuroradiology, who discussed each case and diagnosis and suggested the appropriate treatment.

⁶⁸Ga-DOTA

The preparation of ⁶⁸Ga-DOTA was performed in a clean room using fully automated GMP-compliant synthesis module (Modular-Lab PharmTracer, Eckert & Ziegler) with low bioburden single-use cassettes (supplied by Eckert & Ziegler, EUROTOPE GmbH). Isotonic saline, sodium hydrogen phosphate solution pH 7 (solution for infusion, Braun®) and ⁶⁸Ge/⁶⁸Ga generator (Eckert & Ziegler, EUROTOPE GmbH) were connected to the cassette. The reaction vessel was preloaded with 99 nmol 1,4,7,10-Tetraazacyclododecane-1,4,7,10-tetraacetic acid (DOTA) in 470 μ L sodium acetate buffer (pH 4.5). [⁶⁸Ga]GaCl₃ (860 MBq) was pre-concentrated on strong cation exchange cartridge and eluted with NaCl/HCl into reaction vessel and the radiosynthesis was carried out at 95 °C for 500 seconds. The resulting solution was cooled down, diluted with isotonic saline, neutralized with sodium hydrogen phosphate solution (pH 7) and passed through a 0.22 μ m sterile membrane filter into a capped sterile vial. Subsequently, aliquots were taken for quality control (QC) and sterility tests. The QC process was performed in adherence to European Pharmacopeia standards and according to standard operating procedures including filter integrity, pH test, limulus amoebocyte lysate (LAL), radionuclide identity and purity test by determining half-life and energy spectrum. Radiochemical purity (≥ 98 %) was identified by radio-TLC. The sterility

tests were conducted by an independent institution (Biochem GmbH, Karlsruhe) according to Ph. Eur. and USP using direct inoculation method.

PET Acquisition

All PET scans were acquired on a fully digital PET/CT system (Vereos, Philips Healthcare, The Netherlands) at 1, 3 and 5 hours after lumbar intrathecal injection of ^{68}Ga -DOTA (about 45-50 MBq in 0.5-1.0 ml volume) under strictly sterile conditions (usually, an atraumatic 21 G spinal needle was used) in a sitting position aiming at the lumbar levels 3/4. After injection, patients were asked to remain in their beds until scanning in supine position and not to void their bladders until the 1-h scan was completed (return to bed afterwards). From the decay-corrected total radioactivity within the whole-body scan at 1 h, the net intrathecally injected dose was estimated to be 38.1 ± 10.2 MBq.

PET/CT scans were acquired in caudocranial direction covering the body from bladder to head (except in one patient in whom the scan was confined to the base of the skull). Scan time was 2.0 min (1-h and 3-h scan) and 3.0 min (5-h scan) per bed position (16.4 cm) with an overlap of 39%. Ultra-lose-dose (100 kV and 15 mAs) and lose-dose (120 kV and 23 mAs) CT scans for attenuation correction and anatomical correlation were acquired at 1 and 5 h, and 3 h, respectively. Care was taken to re-position the patients as good as possible to allow for a co-registration of all three datasets (i.e., strictly aligned to the bed axis, arms held up, same head and knee rests, etc.). Fully corrected PET datasets were reconstructed employing the vendor-specific, line-of-response, time-of-flight, ordered-subsets, 3-dimensional iterative reconstruction algorithm using spherically symmetric basis functions (so-called blob ordered subset time-of-flight reconstruction; number of iterations, 3; number of subsets, 9; no gaussian postfiltering; resulting voxel size, 2.0 x 2.0 x 2.0 mm; resolution recovery with point spread function: number of iterations, 2; regularization kernel: 6 mm).

Because of clinical or logistics needs the actual start times of PET scans may slightly deviate from the planned scan times (59.8 ± 7.1 min, 183.1 ± 4.7 min and 305.9 ± 13.8 min, respectively; relevant deviations occurred in 3 scans in one patient each, who were scanned at 30 and 35 min instead of 1 h and

375 min instead of 5 h). For reasons of simplicity, we will nevertheless refer to the consecutive scans as 1-h, 3-h and 5-h scans.

Visual PET Reads

Two Nuclear Medicine physicians with long-lasting experience in neuroimaging, who were blinded to all other clinical and diagnostic data as well as the results of quantitative PET analyses (see below), re-evaluated all ^{68}Ga -DOTA-PET scans independently. Using maximum intensity projections (individually scaled for optimal display) and cross-sectional images (uniform display: inverted grey scale, SUV minimum and maximum fixed to 0 and 40 g/ml) of the 1-h, 3-h and 5-h PET/CT datasets, visual reads of direct and indirect RC signs and a summary rating were done as follows:

Directs signs of spinal CSF leak include uni- or bilateral paraspinal, extradural tracer accumulation, which was localized according to 28 spinal segments (defined by 24 vertebral bodies including the caudal adjacent intervertebral space plus 1 suboccipital and 3 sacral segments) and graded in 3 steps (0, none; 1, questionable/mild signal; 2, strong signal) at each time point. To be counted as a positive site of tracer egression, this had to be witnessed at least at one time point. In case of extradural tracer accumulation on multiple consecutive segments, these were rated in combination (assuming that they stem from the same process and to reduce the data). Of note, findings were carefully separated from prominent dural sleeves (in particular, lumbar), intact meningeal diverticula and Tarlov cysts.

Indirect signs of spinal CSF leak include radiotracer accumulation in the bladder (1-h scan only) and radiotracer accumulation in the basal cisterna and over the cerebral convexities. Again, a 3-step scale was employed (see above). As very low tracer accumulation in the neurocranium can hardly be differentiated from scattered photons, the signal level of the arms (i.e., scattered activity; positioned next to the head) was used as threshold. In addition, the raters assessed iatrogenic tracer extravasation at the injection site confined to the trajectory of the needle (rated in 3 steps).

Finally, a 3-step summary rating was recorded by each rater for each individual case considering all aforementioned findings (i.e., 0, 1 and 2 for no, questionable/possible and probable CSF leakage, respectively, including the segment, if identified).

After both raters performed independent ratings in separate sessions, they discussed discrepant cases and reached a consensus on the localization of CSF egression (if differing by more than 1 segment) and the summary rating. We calculated the mean score of both raters for all other ratings (i.e., magnitude of indirect signs and tracer accumulation).

Quantitative PET Analysis

The time course of total radioactivity within the CSF space was characterized in terms of biological half-life ($T_{1/2, \text{biol}}$) and, as a simplified approach, using the ratio of total radioactivity within the CSF space at 5 h and 3 h (referred to as R5/3; using data decay-corrected to the time of injection). Analyses were performed as follows using PMOD (Version 3.7; PMOD Technologies LLC, Switzerland):

First, the individual 1-h and 5-h PET scans were automatically co-registered to the patient's 3-h scan (rigid matching with a normalized mutual information algorithm as implemented in PMOD). Then individual whole-body and CSF-space volumes of interest (VOI) were defined as rectangular regions covering the entire dataset (VOI_{wb}) and CSF space (VOI_{CSF} ; from head to sacral region, carefully excluding extradural activity due to leakage and, for instance, urinary excretion), respectively. These VOI were applied to all individual datasets (and possibly manually corrected if not sufficiently fitting the 1-h and 5-h dataset) to assess decay-corrected total radioactivity within each VOI and time point. Since patients were asked not to void their bladder before the 1-h scan, decay-corrected total radioactivity in the 1-h scan can be assumed to reflect the total amount of ^{68}Ga -DOTA injected into the CSF space (see above). Finally, the decay-corrected total radioactivity within VOI_{CSF} in the 1-h, 3-h and 5-h scans was used to estimate $T_{1/2, \text{biol}}$ by a mono-exponential fit (using actual scan times; see small variations in scan time mentioned above), while R5/3 was calculated directly from total radioactivity within the 3-h and 5-h scans (we also linearly extrapolated R5/3 from actual scan times, but given the small variations this had no relevant effect on overall

results). We did not include the net injected dose (i.e., VOI_{CSF} at 0 h) into the fit of $T_{1/2,biol}$ because the radiopharmaceutical needs some time to distribute along the dural space in caudocephal direction and to reach the putative site of leakage. In turn, at 1 hour after injection, the radiotracer usually covers the entire spinal axis (see Results), allowing us to approximate $T_{1/2,biol}$ by a simple mono-exponential fit.

Statistical Analysis

Correlations between continuous and ordinal variables were assessed by Pearson's r (parametric) and Spearman's ρ (non-parametric) correlation coefficients, as appropriate. We checked for a dependency of visual ratings (direct and indirect signs, averaged across raters) on scan time, presence/absence of spinal CSF leakage and their interaction by analysis of covariance including subject ID as random effect. The association between epidemiological variables, qualitative and quantitative PET analyses and the presence or absence of a spinal CSF leak (see reference standard) was investigated by two-sample t test (continuous data) or Wilcoxon test (Mann-Whitney U test; ordinal data). Given the novelty of the presented methodology and the exploratory nature of the present study, we employed no correction for multiple testing. However, we drastically reduced the number of variables by averaging over raters, sites and time points. In case of significant findings, a receiver operating characteristics (ROC) analysis was performed to assess the diagnostic performance of the respective PET parameter by the area under the ROC curve (AUC_{ROC}). The optimal diagnostic cut-off point was defined by the maximum Youden's index. Finally, in an exploratory analysis we used stepwise forward regression with minimum corrected Akaike Information Criterion (AIC) to choose the best model for prediction of spinal CSF leakage. All analyses were done with JMP (Version 11.0.0, SAS Institute Inc., USA).

METHODS

Visual PET Reads – Inter-rater Agreement

Visual reads of direct signs of a spinal CSF leak were highly consistent between both raters: Both investigators rated 11 patients each to show no direct evidence of tracer egression. In 10 cases the rating

was unanimously. In one case each, the other rater missed one and two sites of tracer egression, respectively, according to their final consensus. In the remaining 27 patients both raters agreed that the patients showed at least one direct sign of tracer egression. Their rating was unanimously positive for 46 sites and differed either in location by more than 1 segment or presence of tracer egression in 7 sites. Taken together, the raters agreed in 56/66 (86%) of ratings.

Ratings of indirect signs of CSF leakage and tracer extravasation at the injection site were also highly consistent between observers: Concerning the rating of radiotracer accumulation in the bladder (1-h scan only), in the basal cisterna and over the cerebral convexities (n = 1 patient's head not within the field of view) both raters agreed in 33/39 (85%), 91/114 (80%) and 95/114 (83%) of ratings and only rarely differed by more than one point (one basal cisterna and cerebral convexity rating each). The same is true for the rating of the tracer extravasation at the injection site (99/117 [85%]).

Both raters also filed a summary score considering all direct and indirect signs. These ratings were highly consistent (complete agreement in 30/39 [77%] of ratings, differing by 2 in only one case). Both observers' ratings showed highly significant groups differences with rater 1 yielding a slightly higher diagnostic performance for separation of patients without and with verified spinal CSF leak (rater 1: 0.52 ± 0.68 vs. 1.52 ± 0.72 , $p = 0.0003$, AUC ROC = 0.82; rater 2: 0.38 ± 0.67 vs. 1.28 ± 0.89 , $p = 0.0022$, AUC ROC = 0.76).

Time course of direct and indirect RC signs

Sites of extrathecal tracer accumulation at the craniocervical junction were more pronounced at later time points; however, this failed to reach statistical significance given the small number (n=3; 1-h, 3-h and 5-h scan: 0.50 ± 0.50 , 1.67 ± 0.58 and 1.33 ± 0.58 , respectively). Findings at the cervicothoracic junction showed no dependency on time (n=14; 1-h, 3-h and 5-h scan: 0.96 ± 0.77 , 1.11 ± 0.59 and 0.82 ± 0.64), whereas those in the lower thoracic spine ($p=0.0081$; n=12: 1.54 ± 0.58 , 1.21 ± 0.66 and 0.88 ± 0.83 , respectively) and in the lumbosacral region ($p=0.019$; n=22: 1.50 ± 0.67 , 1.43 ± 0.58 and 1.05 ± 0.69 , respectively) showed a

significant decrease with time. Presence/absence of a spinal CSF leak and its interaction with time had no significant effect on the time course in any region.

Ratings of the basal cisterna showed a significant increase with time ($p < 0.0001$; 1-h, 3-h and 5-h scan: 1.41 ± 0.64 , 1.79 ± 0.46 and 1.76 ± 0.46 , respectively) and interaction with the presence/absence of a spinal CSF leak ($p = 0.049$; significant increase with time only in those without CSF leakage). The tracer accumulation over the cerebral hemispheres was highly dependent on time ($p < 0.0001$; 1-h, 3-h and 5-h scan: 0.03 ± 0.11 , 0.62 ± 0.54 and 1.01 ± 0.85 , respectively), presence/absence of a spinal CSF leak ($p = 0.0082$; 0.34 ± 0.51 vs. 0.72 ± 0.80 , across all time points) and their interaction ($p < 0.0001$; significantly steeper increase with time in those without CSF leakage) (Figure 1-4). Finally, the ratings of tracer extravasation at the injection site showed a significant negative association with scan time only ($p = 0.0023$; 1-h, 3-h and 5-h scan: 0.68 ± 0.82 , 0.58 ± 0.75 and 0.44 ± 0.63 , respectively).

Supplemental Table 1: Results of Visual and Quantitative PET Analyses (patients with SIH without previous surgery or alternative causes)

Parameter		w/o leak (<i>n</i> =13)	w/ leak (<i>n</i> =18)	<i>p</i>	<i>ROC AUC</i>
Bladder activity	1 h	1.31±0.66	1.42±0.55	n.s.	-
Basal cisterna	1 h	1.08±0.64	1.53±0.62	n.s.	-
	3 h	1.77±0.44	1.74±0.56	n.s.	-
	5 h	1.69±0.43	1.71±0.56	n.s.	-
Cerebral convexities	1 h	0.00±0.00	0.03±0.12	n.s.	-
	3 h	0.54±0.48	0.50±0.59	n.s.	-
	5 h	1.15±0.92	0.50±0.56	0.0360	0.69
Craniocervical (SO-C1)		0.00±0.00	0.19±0.47	(0.0987)	(0.58)
Cervicothoracic (C6-T2)		0.10±0.25	0.68±0.58	0.0010	0.79
Lower thoracic (T7-T12)		0.45±0.75	0.44±0.64	n.s.	-
Lumbosacral (L2-S2)		0.77±0.82	0.79±0.81	n.s.	-
Consensus summary read		0.54±0.78	1.39±0.78	0.0058	0.77
PET quantification	$T_{1/2, \text{biol}}$ [h]	8.8±5.93	4.54±2.45	0.0345	0.69
	R5/3	0.78±0.18	0.63±0.18	0.0319	0.74

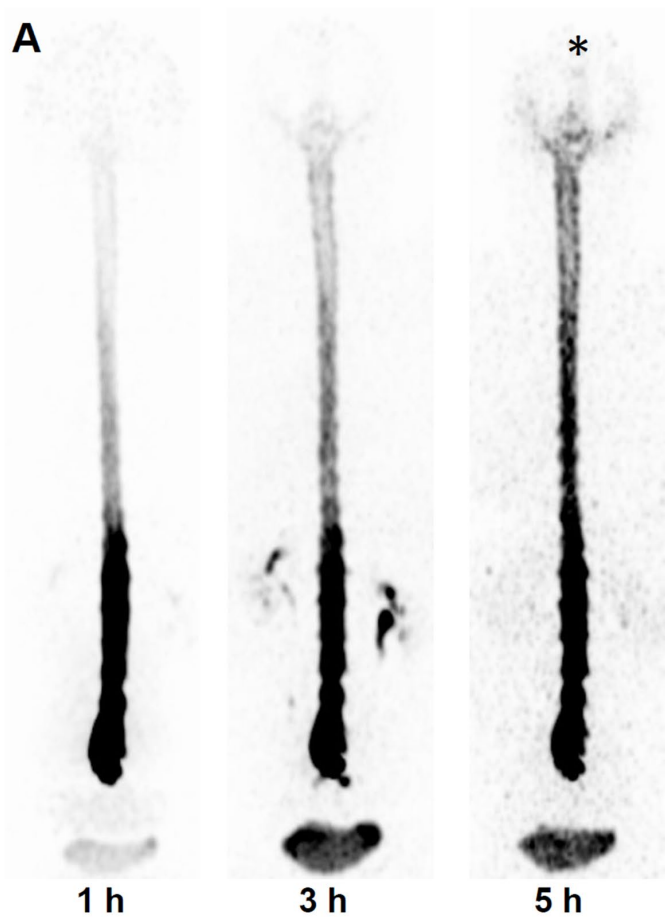
Except for PET quantification, all data represent 3-step ordinal scales with values giving mean values across readers and times (if not separated) or the consensus of raters. Given are mean values ± standard deviation, *p* values of statistical comparisons between patients without (w/o) and with (w/) spinal CSF leak (n.s., not significant, *p* values in parenthesis indicate trend effects) and area under the receiver operating characteristics curve (*ROC AUC*; only for significant and trend effects). Anatomical localizations refer to sites of tracer accumulation (spinal segments; SO, suboccipital). SIH, spontaneous intracranial hypotension.

No.	Leak	Injection Site			Bladder 1h	Basal Cisterna			Convexities			Cervical							Thoracic							Lumbar					Sacral			Consensus Summary	PET Quantification										
		1h	3h	5h		1h	3h	5h	1h	3h	5h	S0	C1	C2	C3	C4	C5	C6	C7	T1	T2	T3	T4	T5	T6	T7	T8	T9	T10	T11	T12	L1	L2		L3	L4	L5	S1	S2	S3	T _{1/2,biol} [h]	R5/3			
14	0	0	0	0	0	2	2	2	0	1.5	2	0	0	0	0	0	0	0	0	0	0	0	0	0	0	0	0	0	0	0	0	0	0	0	0	0	0	0	0	0	28.27	0.98			
9	0	0	0	0	2	1	2	2	0	1	2	0	0	0	0	0	0	0	0	0	0	0	0	0	0	0	0	0	0	0	0	0	0	0	0	0	0	0	0	14.76	0.96				
23	0	1	1	1	1	2	2	2	0	1	2	0	0	0	0	0	0	0	0	0	0	0	0	0	0	0	0	0	0	0	0	0	0	0	0	0	0	0	0	13.78	0.90				
37	0	0	0	0	1	1	2	2	0	1	2	0	0	0	0	0	0	0	0	0	0	0	0	0	0	0	0	0	0	0	0	0	0	0	0	0	0	0	0	13.75	0.96				
20	0	0	1	1	0.5	1	2	2	0	1	2	0	0	0	0	0	0	0	0	0	0	0	0	0	0	0	0	0	0	0	0	0	0	0	0	0	0	0	0	13.06	0.83				
7	0	0	0	0	0	1	2	2	0	1	2	0	0	0	0	0	0	0	0	0	0	0	0	0	0	0	0	0	0	0	0	0	0	0	0	0	0	0	0	12.76	0.96				
15	0	2	1.5	1	1	1	2	2	0	1	2	0	0	0	0	0	0	0	0	0	0	0	0	0	0	0	0	0	0	0	0	0	0	0	0	0	0	0	0	10.07	0.85				
40	0	0.5	1	0.5	1	0	1	1	0	0	0	0	0	0	0	0	0	0	0	0	0	0	0	0	0	0	0	0	0	0	0	0	0	0	0	0	0	0	0	9.63	0.85				
21	0	0.5	0	0	1.5	2	2	2	0	1	2	0	0	0	0	0	0	0	0	0	0	0	0	0	0	0	0	0	0	0	0	0	0	0	0	0	0	0	0	9.02	0.86				
1	0	0	0	0	2	1	2	2	0	1	2	0	0	0	0	0	0	0	0	0	0	0	0	0	0	0	0	0	0	0	0	0	0	0	0	0	0	0	0	5.96	0.80				
38	0	1	1	1	2	2	2	2	0	1	2	0	0	0	0	0	0	0	0	0	0	0	0	0	0	0	0	0	0	0	0	0	0	0	0	0	0	0	0	0	4.92	0.83			
24	0	0.5	0.5	0	2	2	2	1.5	0	0	0.5	0	0	0	0	0	0	0	0	0	0	0	0	0	0	0	0	0	0	0	0	0	0	0	0	0	0	0	0	0	2.53	0.50			
35	0	2	2	1.5	0.5	1.5	2	2	0.5	1.5	2	0	0	0	0	0	0	0	0	0	0	0	0	0	0	0	0	0	0	0	0	0	0	0	0	0	0	0	0	0	0	0	0		
31	0	2	2	2	2	0	1	1	0	0.5	1	0	0	0	0	0	0	0	0	0	0	0	0	0	0	0	0	0	0	0	0	0	0	0	0	0	0	0	0	0	0	0	0		
28	0	0	0	0	1	1	2	2	0	1	2	0	0	0	0	0	0	0.7	0.7	0	0	0	0	0	0	0	0	0	0	0	0	0	0	0	0	0	0	0	0	0	1	20.76	0.94		
5	0	2	2	1.5	2	2	2	2	0	0.5	2	0	0	0	0	0	0	0	0	0	0	0	0	0	0	0	0	0	0	0	0	0	0	0	0	0	0	0	0	0	1	2.73	0.72		
26	0	1.5	1	1.5	2	2	2	2	0	0.5	1.5	0	0	0	0	0	0	0	0	0	0	0	0	0	0	0	0	0	0	0	0	0	0	0	0	0	0	0	0	0	0	1	2.67	0.65	
29	0	0	0	0	1	1	1.5	2	0	0.5	1	0	0	0	0	0	0	0	0	0	0	0	0	0	0	0	0	0	0	0	0	0	0	0	0	0	0	0	0	0	0	1	2.67	0.63	
8	0	2	2	1	1.5	1	2	1.5	0	0	0	0	0	0	0	0	0	0	0	0	0	0	0	0	0	0	0	0	0	0	0	0	0	0	0	0	0	0	0	0	1	1.53	0.45		
3	0	0	0	0	0.5	2	2	2	0	0	0	0	0	0	0	0	0	0	0	0	0	0	0	0	0	0	0	0	0	0	0	0	0	0	0	0	0	0	0	0	0	2	7.51	0.78	
6	0	2	2	0	1	1	1	1	0	0	0	0	0	0	0	0	0	0	0	0	0	0	0	0	0	0	0	0	0	0	0	0	0	0	0	0	0	0	0	0	2	3.61	0.66		
36	1	2	1	1	2	2	2	2	0	2	2	0	0	0	0	0	0	0	0	0	0	0	0	0	0	0	0	0	0	0	0	0	0	0	0	0	0	0	0	0	0	0	10.64	0.86	
11	1	0	0	0	1	2	2	2	0	0.5	0.5	0	0	0	0	0	0	0	0	0	0	0	0	0	0	0	0	0	0	0	0	0	0	0	0	0	0	0	0	0	0	0	7.23	0.78	
19	1	0	0	0	1	1	2	2	0.5	1	0.5	0	0	0	0	0	0	0	0	0	0	0	0	0	0	0	0	0	0	0	0	0	0	0	0	0	0	0	0	0	0	0	6.06	0.80	
30	1	1	1	0.5	1	1	1	2	0	0	0	0	0	0	0	0	0	0	0	0	0	0	0	0	0	0	0	0	0	0	0	0	0	0	0	0	0	0	0	0	0	1	4.80	0.63	
4	1	0	0	0	2																																				0	4.02	0.63		
18	1	1	2	2	1	2	2	2	0	1	1	0	0	0	0	0	0	0	0	0	0	0	0	0	0	0	0	0	0	0	0	0	0	0	0	0	0	0	0	0	1	3.01	0.51		
2	1	2	2	1	2	2	2	2	0	1	1	0	0	0	0	0	0	0	0	0	0	0	0	0	0	0	0	0	0	0	0	0	0	0	0	0	0	0	0	0	0	1	2.66	0.60	
33	1	1.5	0.5	0	2	0	0	0	0	0	0	0	0	0	0	0	0	0	0	0	0	0	0	0	0	0	0	0	0	0	0	0	0	0	0	0	0	0	0	0	0	1	0.45	0.09	
25	1	0	0	0	1	2	2	2	0	1	1	0	0	0	0	0	0	0	0	0	0	0	0	0	0	0	0	0	0	0	0	0	0	0	0	0	0	0	0	0	0	2	7.86	0.82	
34	1	0	0	0	1	1	2	1.5	0	0	0	0	0	0	0	0	0	0	0	0	0	0	0	0	0	0	0	0	0	0	0	0	0	0	0	0	0	0	0	0	0	2	6.09	0.75	
17	1	0	0	0	1	1	1	2	0	0	0.5	0	0	0	0	0	0	0	0	0	0	0	0	0	0	0	0	0	0	0	0	0	0	0	0	0	0	0	0	0	0	0	2	5.66	0.74
27	1	0	0	0	2	1	1.5	1.5	0	0	0	0.7	0.7	0	0	0	0	0	0	0	0	0	0	0	0	0	0	0	0	0	0	0	0	0	0	0	0	0	0	0	0	2	5.52	0.72	
22	1	0	0	0	1	1	2	2	0	0	0	0	0	0	0	0	0	0	0	0	0	0	0	0	0	0	0	0	0	0	0	0	0	0	0	0	0	0	0	0	0	2	3.65	0.63	
32	1	0	0	0	0.5	2	2	2	0	0.5	0.5	0	0	0	0	0	0	0	0	0	0	0	0	0	0	0	0	0	0	0	0	0	0	0	0	0	0	0	0	0	0	2	3.45	0.59	
12	1	1.5	0.5	0	2	2	2	2	0	1	1	0	0	0	0	0	0	0	0	0	0	0	0	0	0	0	0	0	0	0	0	0	0	0	0	0	0	0	0	0	0	2	3.34	0.62	
16	1	0	0	0	1	2	2	1	0	0	0	0	0	0	0	0	0	0	0	0	0	0	0	0	0	0	0	0	0	0	0	0	0	0	0	0	0	0	0	0	0	2	2.72	0.46	
10	1	0	0	0	2	2	2	2	0	0.5	0.5	1.3	0	0	0	0	0	0	0	0	0	0	0	0	0	0	0	0	0	0	0	0	0	0	0	0	0	0	0	0	0	2	2.66	0.56	
39	1	0.5	0.5	0.5	2	2	2	1	0	0	0	0	0	0	0	0	0	0	0	0	0	0	0	0	0	0	0	0	0	0	0	0	0	0	0	0	0	0	0	0	0	2	1.97	0.51	

Supplemental Figure 1: Heatmap of CSF-PET findings in patients without (n=21) and with (n=18) verified spinal CSF leak.

Color coding refers to the degree of abnormality (green, normal to red, abnormal). Data is sorted by (i) absence or presence of verified spinal CSF leak (thick horizontal line; segmental height of verified leak is indicated by a thick box), (ii) consensus of visual summary read (Consensus Summary; thin horizontal line) and (iii) biological half-life of the tracer in CSF space ($T_{1/2,biol}$).

Except for absence or presence of a spinal CSF leak (Leak; binary scale) and PET Quantification ($T_{1/2,biol}$ and R5/3; continuous data), all data represent 3-step ordinal scales with values giving mean values across readers and times (if not separated) or the consensus between both raters. Anatomical localizations refer to the sites of tracer accumulation (Convexities, activity over cerebral convexities).



Supplemental Figure 2: Pathological CSF-PET in a patient without verified spinal CSF leak but response to epidural blood patch.

A, maximum intensity projections of PET at 1h, 3h and 5h (posterior view; scaled for optimal display) after injection of ^{68}Ga -DOTA. B, transaxial PET and PET/CT fusion images at the level of the centrum semiovale (5h). Despite that no spinal CSF leak could be verified by comprehensive stepwise neuroradiological work-up, there is an apparent lack of tracer accumulation over the cerebral convexities (asterisk). In addition, the biological half-life of the tracer in the CSF space was very short (2.7 h). The patient (No. 29) was treated by epidural blood patch with improvement of symptoms.

